유한회전을 고려한 공간뼈대의 기하학적 비선형해석

Geometrically Non-Linear Analysis of Space Frames Considering Finite Rotations

주 석 범[1)]
Chu, Seok Beom

요 약 : 본 연구에서는 유한 회전에 의한 효과를 고려한 곡선 보요소를 개발하고, 이 요소를 이용하여 공간뼈대 구조물의 기하학적 비선형 해석을 수행하였다. 이 곡선 보요소는 증분 변위장에 Rodriguez의 2차 유한 회전항을 포함시킴으로써, 유한 회전에 의한 기하학적 평형을 유지하도록 하였다. 대변형 해석을 위하여 Total Lagrangian 방법이 적용되었으며, 비선형 해석을 수행하기 위한 알고리즘으로는, 여러개의 임계점을 갖는 비선형 거동가지도 추적할 수 있도록 하중 및 변위 증분의 조합법이 사용되었다.

공간 뼈대 구조물의 해석 예제를 통하여, 기하학적 비선형 해석에서 발생하는 유한 회전에 의한 효과를 확인하고, 본 연구에서 제안한 유한요소의 효율성 및 비선형 알고리즘으로 선택한 하중 및 변위 증분의 조합법의 적용성을 입증하였다.

핵 심 용 어 : 곡선 보요소, 유한 회전, 기하학적 비선형 해석

1. INTRODUCTION

The development of structural finite elements and associated solutions for non-linear analysis has received a considerable attention since the introduction of computer-oriented analysis. A large number of beam, plate, and shell elements have been proposed for non-linear analysis. Among these elements, the degenerate elements are particularly attractive because of the consistent and general formulation and the computational efficiency.

The curved beam elements, derived from the degenerate shell element of Ahmad et al.,[1)] have been usually taken as a starting point[2-6)] for recent developments of geometrically non-linear analysis. However, these elements suffer from shear locking[7-9)] and membrane locking.[2-4,10-12)] These locking phenomena[13-17)] may be overcome by using high-order elements[10-12)] or resorting to the reduced or selective integration scheme.[18-23)]

1) 정회원, 서울대학교 공학연구소 특별연구원

In the development of structural elements for the post-buckling analysis, the consideration of large rotations introduces additional difficulties due to the non-vectorial nature of finite rotations. In the conventional non-linear formulation of the degenerate beam elements, [24,25] the tangent stiffness matrix is derived by assuming infinitesimal rotation increments and the effect of large rotation increments is considered only during the equilibrium iterations when calculating the stresses. The kinematics of large rotation was studied extensively by Argyris[26] and formulations that take into account the effect of finite rotation increments on the resulting stiffness have been presented by Surana,[27,28] Surana and Sorem,[29] Dvorkin et al.,[30] Simo,[31] and Simo and Vu Quoc.[32] However, these studies have not fully investigated the stability and post-buckling behaviors with multiple limit points.

On the other hand, many methods have been proposed to solve limit-point problems and there are a number of numerical algorithms such as the arc-length method,[33-35] and the automatic combination algorithm of the load and displacement incremental method.[36-38]

This study concentrates on the non-linear formulations of the degenerate beam elements considering the effect of second order terms of Rodriguez's finite rotations. The combined load/displacement incremental method is adopted to trace the entire equilibrium path including multiple limit points. The effects of second order rotations in evaluating tangent stiffness matrices are investigated through the numerical examples focused on the strongly geometrically non-linear analysis of space frames using the degenerate beam element.

2. KINEMATICS OF THE DEGENERATE BEAM ELEMENT

This study concentrates on the geometrically non-linear formulation based on the C° curved beam element with arbitrary rectangular cross section. The isoparametric curved beam element is employed to derive the incremental equilibrium equation governing the large deformation behavior of space frames. The present element formulation takes into account the effect of second order terms of Rodriguez's finite rotations in the incremental displacement field.

Figure 1 shows the kinematics of a curved beam element with rectangular cross section. At each node we define the orthonormal system ${}^{o}V_r^k$, ${}^{o}V_s^k$, ${}^{o}V_t^k$, where ${}^{o}V_r^k$ is the tangent vector to the element axis.

The kinematic hypotheses in this formulation are as follows

1. plane sections originally normal to the center line axis at the initial state remain plane during the deformation but not necessarily normal to the deformed axis due to shear deformations, and

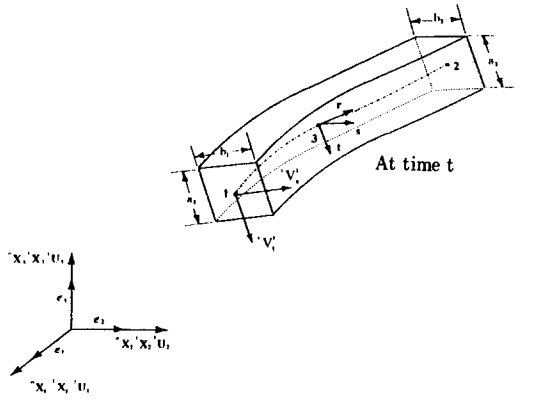

FIG. 1 Beam Element Undergoing Large Displacements and Rotations

2. the cross section of the beam is not deformed.

Using the natural coordinate system (r, s, t), the position vector components $({}^{o}X_i)$ of an arbitrary point inside the beam element in the initial configuration can be expressed as

$$ {}^{o}X_i = \sum_{k=1}^{n} N_k \, {}^{o}X_i^k + \frac{s}{2}\sum_{k=1}^{n} b_k N_k \, {}^{o}V_{si}^k + \frac{t}{2}\sum_{k=1}^{n} a_k N_k \, {}^{o}V_{ti}^k \tag{1} $$

where the $N_k(r)$ are the isoparametric interpolation functions at the nodal point k and their detailed expressions can be found elsewhere.[24] a_k and b_k are cross-sectional dimensions of the beam, and ${}^{o}V_{ti}^k$ and ${}^{o}V_{si}^k$ are direction cosines of normal vectors at nodal point k, respectively.

Similarly, the position vector at the current state is given by

$$ {}^{t}X_i = \sum_{k=1}^{n} N_k \, {}^{t}X_i^k + \frac{s}{2}\sum_{k=1}^{n} b_k N_k {}^{t}V_{si}^k + \frac{t}{2}\sum_{k=1}^{n} a_k N_k {}^{t}V_{ti}^k \tag{2} $$

Using equations (1) and (2), the total displacement of the same point corresponding to the configuration at time t is obtained as

$$ \begin{aligned} {}^{t}U_i &= {}^{t}X_i - {}^{o}X_i \\ &= \sum_{k=1}^{n} N_k \, {}^{t}U_i^k + \frac{s}{2}\sum_{k=1}^{n} b_k N_k ({}^{t}V_{si}^k - {}^{o}V_{si}^k) \\ &\quad + \frac{t}{2}\sum_{k=1}^{n} a_k N_k ({}^{t}V_{ti}^k - {}^{o}V_{ti}^k) \end{aligned} \tag{3} $$

and, similarly, the incremental displacement is

$$ \begin{aligned} \overline{U}_i &= {}^{t+\Delta t}X_i - {}^{t}X_i \\ &= \sum_{k=1}^{n} N_k \, {}^{t+\Delta t}U_i^k + \frac{s}{2}\sum_{k=1}^{n} b_k N_k ({}^{t+\Delta t}V_{si}^k - {}^{t}V_{si}^k) \\ &\quad + \frac{t}{2}\sum_{k=1}^{n} a_k N_k ({}^{t+\Delta t}V_{ti}^k - {}^{t}V_{ti}^k) \end{aligned} \tag{4} $$

Since to go from the configuration at time t to the configuration at time $t+\Delta t$ the orthonormal system at node k is only rotated, the direction cosines at time $t+\Delta t$ can be transformed to those at time t using the rotation matrix ${}_{t}^{t+\Delta t}R_k$.

$$ {}^{t+\Delta t}V_r^k = {}_{t}^{t+\Delta t}R_k \, {}^{t}V_r^k \tag{5a} $$

$$ {}^{t+\Delta t}V_s^k = {}_{t}^{t+\Delta t}R_k \, {}^{t}V_s^k \tag{5b} $$

$$ {}^{t+\Delta t}V_t^k = {}_{t}^{t+\Delta t}R_k \, {}^{t}V_t^k \tag{5c} $$

Considering the Rodriguez's finite rotations, the rotational matrix corresponding to node k is as follows:

$$ {}_{t}^{t+\Delta t}R_k = I_3 + \frac{\sin\theta^k}{\theta^k}\Theta^k + \frac{1}{2}\left[\frac{\sin(\theta^k/2)}{(\theta^k/2)}\right]^2 (\Theta^k)^2 \tag{6} $$

where

$$ \theta^k = [\,(\theta_1^k)^2 + (\theta_2^k)^2 + (\theta_3^k)^2\,]^{1/2} \tag{7} $$

and

$$ \Theta^k = \begin{bmatrix} 0 & -\theta_3^k & \theta_2^k \\ \theta_3^k & 0 & -\theta_1^k \\ -\theta_2^k & \theta_1^k & 0 \end{bmatrix} \tag{8} $$

Argyris[26] proved that equation (6) can be rewritten as

$$ {}_{t}^{t+\Delta t}R^k = I_3 + \Theta^k + \frac{1}{2!}(\Theta^k)^2 + \frac{1}{3!}(\Theta^k)^3 + \cdots \tag{9} $$

In a usual formulation, the incremental rotations are assumed to be infinitesimal and only the linear terms of the incremental rotations are retained. However, because the incremental rotations are assumed to be finite, both the linear terms and the quadratic terms should be included in the incremental displacement equation. Substituting equation (9) into (5) and neglecting higher order terms than the second order term, the following equations are obtained

$$ {}^{t+\Delta t}V_{ri}^k - {}^tV_{ri}^k \cong -{}^tV_{ti}^k\,\theta_2^k + {}^tV_{si}^k\,\theta_3^k \qquad (10a) $$
$$ +\frac{1}{2}[\,-{}^tV_{ri}^k(\theta_2^{k2}+\theta_3^{k2}) + {}^tV_{si}^k\,\theta_1^k\,\theta_2^k + {}^tV_{ti}^k\,\theta_1^k\,\theta_3^k\,] $$
$$ {}^{t+\Delta t}V_{si}^k - {}^tV_{si}^k \cong -{}^tV_{ri}^k\,\theta_3^k + {}^tV_{ti}^k\,\theta_1^k \qquad (10b) $$
$$ +\frac{1}{2}[\,{}^tV_{ri}^k\,\theta_1^k\,\theta_2^k - {}^tV_{si}^k(\theta_2^{k2}+\theta_3^{k2}) + {}^tV_{ti}^k\,\theta_2^k\,\theta_3^k\,] $$
$$ {}^{t+\Delta t}V_{ti}^k - {}^tV_{ti}^k \cong -{}^tV_{si}^k\,\theta_1^k + {}^tV_{ri}^k\,\theta_2^k \qquad (10c) $$
$$ +\frac{1}{2}[\,{}^tV_{ri}^k\,\theta_1^k\,\theta_3^k + {}^tV_{si}^k\,\theta_2^k\,\theta_3^k + {}^tV_{ti}^k(\theta_1^{k2}+\theta_2^{k2})] $$

Resultantly, by substituting equation (10) into (3), the incremental displacement can be obtained as

$$ \overline{U}_i = U_i + U_i^* \qquad (11) $$

where U_i and U_i^* are the conventional linear term and the extra quadratic term due to the finite rotations, respectively, and the detailed expressions are as follows

$$ U_i = \sum_{k=1}^{n} N_k\,U_i^k + \frac{s}{2}\sum_{k=1}^{n} b_k N_k(-{}^tV_{ri}^k\,\theta_3^k + {}^tV_{ti}^k\,\theta_1^k) + \frac{t}{2}\sum_{k=1}^{n} a_k N_k(-{}^tV_{si}^k\,\theta_1^k + {}^tV_{ri}^k\,\theta_2^k) \qquad (12) $$

and

$$ U_i^* = \frac{s}{2}\sum_{k=1}^{n} b_k\,N_k\frac{1}{2}[\,{}^tV_{ri}^k\theta_1^k\theta_2^k - {}^tV_{si}^k(\theta_1^{k2}+\theta_3^{k2}) + {}^tV_{ti}^k\theta_2^k\theta_3^k\,] + \frac{t}{2}\sum_{k=1}^{n} a_k\,N_k\frac{1}{2}[\,{}^tV_{ri}^k\theta_1^k\theta_3^k + {}^tV_{si}^k\theta_2^k\theta_3^k + {}^tV_{ti}^k(\theta_2^{k2}+\theta_3^{k2})\,] \qquad (13) $$

The above equations are the basic expressions that are used to establish the strain-displacement matrices for non-linear analysis of space frames. In the conventional formulation, the linear and non-linear strain-displacement transformation matrices may be obtained by neglecting the second order rotational terms from equations (1) to (13). The detailed expressions of strain and stress vectors, the stress matrix and the constitutive matrix considering finite rotations are given in Appendix.

3. INCREMENTAL EQUILIBRIUM EQUATION CONSIDERING FINITE ROTATIONS

Virtual work principle for the general continuum is expressed as,

$$ \int_{{}^oV} {}_o^{t+\Delta t}S_{ij} \cdot \delta({}_o^{t+\Delta t}\varepsilon_{ij})\,{}^odV = {}_o^{t+\Delta t}R = \int_{{}^oS} {}_o^{t+\Delta t}T_i\,\delta\,{}_o^{t+\Delta t}U_i\,{}^o ds \qquad (14) $$

where

$$ {}_o^{t+\Delta t}\varepsilon_{ij} = \frac{1}{2}({}_o^{t+\Delta t}U_{i,j} + {}_o^{t+\Delta t}U_{j,i} + {}_o^{t+\Delta t}U_{k,i}\,{}_o^{t+\Delta t}U_{k,j}) \qquad (15) $$

In these formulae, ${}_o^{t+\Delta t}S_{ij}$ and ${}_o^{t+\Delta t}\varepsilon_{ij}$ are the second Piola-Kirchhoff stress and the Green-Lagrange strain at time $t+\Delta t$ referred to the

configuration at time o, respectively: ${}^{t+\Delta t}U_i$ is the total displacement vector; ${}^{t+\Delta t}T_i$ is the surface force.

For an incremental analysis, incremental equations of stresses, strains and surface forces are

$$ {}^{t+\Delta t}_{o}S_{ij} - {}^{t}_{o}S_{ij} = {}_{o}S_{ij} \tag{16} $$

$$ {}^{t+\Delta t}_{o}\varepsilon_{ij} - {}^{t}_{o}\varepsilon_{ij} = {}_{o}\varepsilon_{ij} \tag{17} $$

$$ {}^{t+\Delta t}T_i - {}^{t}T_i = T_i \tag{18} $$

where the superscripts o, t and $t+\Delta t$ represent the initial, current and deformed variables. The incremental variables have no superscripts. The incremental displacement components at time t and $t+\Delta t$ are

$$ {}^{t+\Delta t}U_i = {}^{t}U_i + U_i + U_i^* \tag{19} $$

where U_i denotes the first order terms of the displacement parameters and U_i^* denotes the second order terms due to large rotations, and their sum consists of incremental displacement. Substituting equation (19) into equation (15) and neglecting higher order terms, the incremental equation of strains is expressed as

$$ {}^{t+\Delta t}_{o}\varepsilon_{ij} - {}^{t}_{o}\varepsilon_{ij} = {}_{o}e_{ij} + {}_{o}\eta_{ij} + {}_{o}e^*_{ij} \tag{20} $$

where

$$ {}_{o}e_{ij} = \frac{1}{2}({}_{o}U_{i,j} + {}_{o}U_{j,i} + {}^{t}_{o}U_{k,i}\,{}_{o}U_{k,j} + {}_{o}U_{k,i}\,{}^{t}_{o}U_{k,j}) \tag{21a} $$

$$ {}_{o}\eta_{ij} = \frac{1}{2}\,{}_{o}U_{k,i}\,{}_{o}U_{k,j} \qquad i, j, k = 1, 2, 3 \tag{21b} $$

$$ {}_{o}e^*_{ij} = \frac{1}{2}({}_{o}U^*_{i,j} + {}_{o}U^*_{j,i} + {}^{t}_{o}U_{k,i}\,{}_{o}U^*_{k,j} + {}_{o}U^*_{k,i}\,{}^{t}_{o}U_{k,j}) \tag{21c} $$

The ${}_{o}e_{ij}$ and ${}_{o}\eta_{ij}$ are the conventional linear and non-linear Green-Lagrange strain increment respectively, and ${}_{o}e^*_{ij}$ is the linear strain increment due to U_i^*.

Substituting equation (20) into equation (14), neglecting the higher order terms and considering equation (16), the incremental equations of equilibrium[24] for a general continuum in the total Lagrangian formulation is expressed as

$$ \int_V ({}_{o}C_{ijrs}\,{}_{o}e_{rs}\,\delta_{o}e_{ij} + {}^{t}_{o}S_{ij}\delta_{o}\eta_{ij} + {}^{t}_{o}S_{ij}\delta_{o}e^*_{ij})^{o}dV = {}^{t+\Delta t}R - \int_V {}^{t}_{o}\bar{S}_{ij}\delta_{o}e_{ij}{}^{o}dV \tag{22} $$

where ${}_{o}C_{ijrs}$ are the incremental constitutive tensors at time t referred to the configuration at time o. In this formula, the first term gives the element elastic stiffness and the last term the element nodal force, whereas the geometric stiffness results from the contribution of non-linear strains, i.e. the second and third terms.

Since each term of equation (22) is scalar, equation (22) can be rewritten in the local coordinate system as follows:

$$ \int_V ({}_{o}C_{\alpha\beta\gamma\delta}\,{}_{o}e_{\gamma\delta}\delta_{o}e_{\alpha\beta} + {}^{t}_{o}S_{\alpha\beta}\delta_{o}\eta_{\alpha\beta} + {}^{t}_{o}S_{\alpha\beta}\delta_{o}e^*_{\alpha\beta})^{o}dV = {}^{t+\Delta t}R - \int_V {}^{t}_{o}S_{\alpha\beta}\delta_{o}e_{\alpha\beta}{}^{o}dV \tag{23} $$

where

$$ {}_{o}e_{\alpha\beta} = \frac{1}{2}\,({}_{o}U_{\alpha,\beta} + {}_{o}U_{\beta,\alpha} + {}^{t}_{o}U_{\gamma,\alpha}\,{}_{o}U_{\gamma,\beta} + {}_{o}U_{\gamma,\alpha}\,{}^{t}_{o}U_{\gamma,\beta}) \tag{24a} $$

$$ {}_{o}\eta_{\alpha\beta} = \frac{1}{2}\,{}_{o}U_{\gamma,\alpha}\,{}_{o}U_{\gamma,\beta} \qquad \alpha, \beta, \gamma = r, s, t \tag{24b} $$

$$ {}_{o}e^*_{\alpha\beta} = \frac{1}{2}\,({}_{o}U^*_{\alpha,\beta} + {}_{o}U^*_{\beta,\alpha} + {}^{t}_{o}U_{\gamma,\alpha}\,{}_{o}U^*_{\gamma,\beta} + {}_{o}U^*_{\gamma,\alpha}\,{}^{t}_{o}U_{\gamma,\beta}) \tag{24c} $$

In this formulae, the greek subscripts mean the variables in the local coordinate system. Applying the second order tensor transformation between the global and local coordinate systems, each strain components of equation (24) can be obtained as follows:

$$ {}_oU_{\alpha,\beta} = T_{i\alpha}\, T_{j\beta}\, {}_oU_{i,j} \tag{25a} $$

$$ {}^t_oU_{\alpha,\beta} = T_{i\alpha}\, T_{j\beta}\, {}^t_oU_{i,j} \tag{25b} $$

$$ {}_oU^*_{\alpha,\beta} = T_{i\alpha}\, T_{j\beta}\, {}_oU^*_{i,j} \tag{25c} $$

In matrix notation, equations (23) can be rewritten as

$$ \int_V ({}_oE_L^T\, {}_oC\, \delta_o E_L + {}_oE_{NL}^T\, {}^t_oS\, \delta_o E_{NL} + {}^t_o\bar{S}\ \delta_o E^*_{NL})\, {}^o dV = {}^{t+\Delta t}R - \int_V {}^t_o\bar{S}^T \delta_o E_L\, {}^o dV \tag{26} $$

where ${}_oE_L$ and ${}_oE_{NL}$ are the linear and the non-linear incremental strain vectors, respectively, and ${}_oE^*_{NL}$ is the linear strain increment vector due to U_i^*; ${}^t_oS$ the stress matrices; ${}^t_o\bar{S}$ the stress vectors; ${}_oC$ represents the incremental constitutive matrix. The detailed expressions can be found in Appendix.

From the strain-displacement relationship, the non-linear strain vector ${}^t_oE_{NL}$ can be expressed as follows,

$$ {}^t_oE_{NL} = {}^t_oB_{NL}\, U_e \tag{27} $$

where ${}^t_oB_{NL}$ and U_e is the non-linear strain-displacement transformation matrix and the nodal displacement vector, respectively.

The linear strain vector ${}^t_oE_L$ is expressed in terms of the linear strain-displacement matrix ${}^t_oB_L$ which consists of ${}^t_oB_{Lo}$ and ${}^t_oB_{L1}$ reflecting the effect of initial displacements.

$$ {}^t_oE_L = {}^t_oB_L\, U_e = ({}^t_oB_{Lo} + {}^t_oB_{L1})U_e \tag{28} $$

Considering equation (24) and (27), ${}^t_oB_{L1}$ is expressed as the product of ${}^t_oB_{NL}$ and ${}^t_oL$

$$ {}^t_oB_{L1} = {}^t_oL \cdot {}^t_oB_{NL} \tag{29} $$

where ${}^t_oL$ is the gradient matrix of total displacements and the detailed expression can be found in Appendix.

Recently, some researchers found that for exact evaluation of the tangent stiffness matrices, the second order terms with respect to the rotational degree of freedom should be added to the non-linear strain terms of the incremental equations. These additional terms in the total Lagrangian (T.L.) formulation are

$$ \int {}^t_oS_{\alpha\beta}\, \delta_o e^*_{\alpha\beta}\, {}^o dV = \int {}^t_o\bar{S}^{\,T}\, {}_oB^*_{NL} \delta U^*_e\, {}^o dV \tag{30} $$

where ${}^t_oB^*_{NL}$ is the strain-displacement transformation matrix due to U_i^*.

Substituting element coordinates and displacement interpolation into equations (27), (28), (29) and (30), the governing finite element equation for a single element in the T.L. formulation can be expressed as

$$ ({}^t_oK_L + {}^t_oK_{NL})\Delta U = {}^{t+\Delta t}R - {}^t_oF \tag{31} $$

where

$$ {}^t_oK_L = \int_V {}^t_oB_L^T\, {}_oC\, {}^t_oB_L\, {}^o dV \tag{32a} $$

$$ {}^t_oK_{NL} = \int_V {}^t_oB_{NL}^T\, {}^t_oS\, {}^t_oB_{NL}\, {}^o dV + {}^t_oK^*_{NL} \tag{32b} $$

$$ {}^t_oF = \int_V {}^t_oB_L^T\, {}^t_o\bar{S}\ {}^o dV \tag{32c} $$

In equations (31) and (32), ${}^{t}_{o}K_{L}$ and ${}^{t}_{o}K_{NL}$ are the linear and the non-linear stiffness matrices, respectively and ${}^{t}_{o}K^{*}_{NL}$ is the geometric stiffness matrices due to second order rotation terms; ΔU the increment of the nodal displacement vector; ${}^{t}_{o}F$ the nodal force vectors equivalent to the element stresses at time t. The scheme calculating the nodal force vector ${}^{t}_{o}F$ is summarized as follows:

1) The incremental displacement due to the incremental or unbalanced load and the total displacement are computed from equation (31).

2) In the global coordinate, Green-Lagrange strain components corresponding to the total displacement are evaluated at each Gaussian point from equation (15).

3) Using the transformation rule between the global and local coordinate system, Green-Lagrange strain components are evaluated as follows

$$ {}^{t+\Delta t}_{o}\varepsilon_{\alpha\beta} = T_{i\alpha}\, T_{j\beta}\, {}^{t+\Delta t}_{o}\varepsilon_{ij} \tag{33} $$

4) In the local coordinate, the second Piola-Kirchihoff stress components are calculated as

$$ {}^{t+\Delta t}_{o}S_{\alpha\beta} = {}^{t+\Delta t}_{o}C_{\alpha\beta\gamma\delta}\, {}^{t+\Delta t}_{o}\varepsilon_{\gamma\delta} \tag{34} $$

5) Internal nodal forces ${}^{t+\Delta t}F$ is evaluated at each Gaussian point from equation (32c).

4. NUMERICAL EXAMPLES

In order to demonstrate the validity of the present study, the finite element program named NOBA was developed, which can trace the post-buckling behaviors of space frames, using the automatic load/displacement incremental algorithm.[36-38]

To investigate the effects of finite rotations in the geometrically non-linear analysis of the space frames with the degenerate beam elements, the proposed formulation including the effects of finite rotations (the 2nd order formulation) is compared with the formulation assuming infinitesimal rotation increments (the 1st order formulation) through the numerical examples. In the subsequent examples, the 3-node beam elements are used and the geometric and physical properties of each problem are described in the corresponding Figures.

4.1 CANTILEVER UNDER AN END MOMENT

This example is one of the typical non-linear beam problems which can be solved by an analytical method. Figure 2 shows a straight cantilever beam loaded with a moment ($M=fm$) at the free end. Here, f is the load incremental factor, m is the reference moment, and f_s is the shear correction factor. The cantilever is modeled and analyzed by four beam elements. The total moment $M=2.0m$ is applied in ten equal increments.

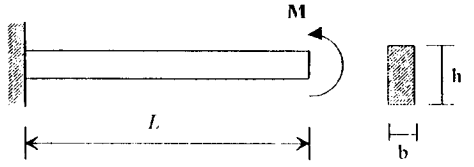

$E = 1.0*10^{7}$, $v = 0.0$, $f_s = 1.2$
$b = 1.2$, $h = 1.0$, $L = 100$
$M=f\,m$, $m=\pi EI/L=31415.93$

FIG. 2 Cantilever under an End Moment

Table 1 shows the load parameter, normalized vertical displacements at the end of the cantilever, and the number of equilibrium iterations in each load step. The results of this study are compared with the analytical solution (see equation (35)) in Table 1. Converged results of both the 1st and 2nd order formulations agree well with the analytic solutions. Table 1 shows that the equilibrium iteration numbers of the 2nd order formulation keeps nearly constant in each load step, but those of the 1st order formulation increases explosively according to the increase of the end moment.

Table 1 Load-Displacement Behavior of the Cantilever Beam under an End Moment

Load Factor f	Analytical Solution	This Study	
		1st Order (Iter.)	2nd Order (Iter.)
0.2	3.042	3.036 (8)	3.039 (8)
0.4	5.497	5.495 (12)	5.498 (8)
0.6	6.945	6.942 (17)	6.945 (8)
0.8	7.198	7.200 (23)	7.202 (6)
1.0	6.366	6.375 (32)	6.388 (6)
1.2	4.790	4.809 (35)	4.824 (6)
1.4	2.976	2.970 (42)	2.982 (6)
1.6	1.375	1.344 (50)	1.353 (6)
1.8	0.338	0.301 (59)	0.306 (6)
2.0	0.000	0.011 (70)	0.008 (6)

Analytical solution :

$$V/L=[1-\cos(ML/EI)]/(ML/EI) \qquad (35)$$

4.2 HINGED RIGHT-ANGLED FRAME

Figure 3 shows a hinged right-angled frame subjected to a force ($P=fp$) at the distance $0.8L$ from the left hinge. Here, f and p are the load incremental factor and the reference load, respectively. Each of the vertical and horizontal members of the frame is divided into five beam elements.

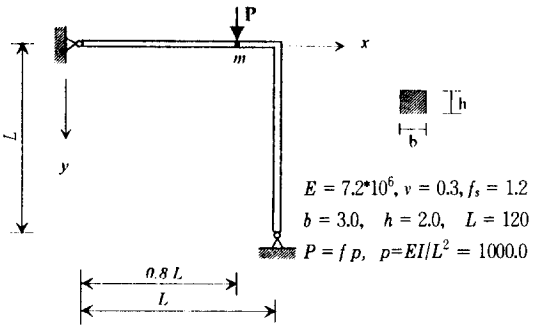

FIG. 3 Hinged Right-Angled Frame under a Point Load at $x = 0.8L$

Figure 4 and 5 display the analyzed results of the load parameter versus the horizontal (D_x) and vertical displacements (D_y) at the point m. This example is solved by Cichon[39] who has developed a beam element with local-global DOF based on a large displacement theory for in-plane frames. Figure 4 shows that the results of this study are in good agreement with those of Cichon.[39] The results of both the 1st order and the 2nd order formulation are compared in Figure 5. This shows that the 2nd order formulation can

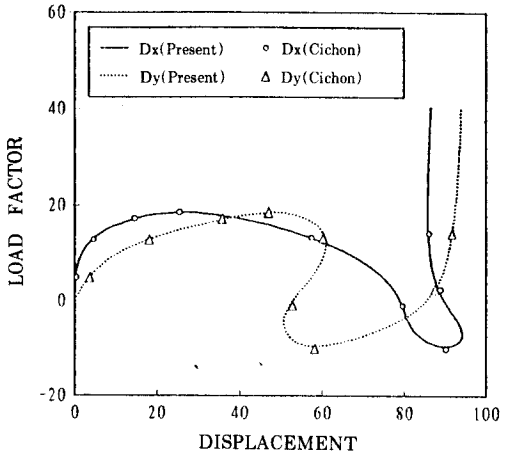

FIG. 4 Load-Displacement Curves of the Frame at Point m

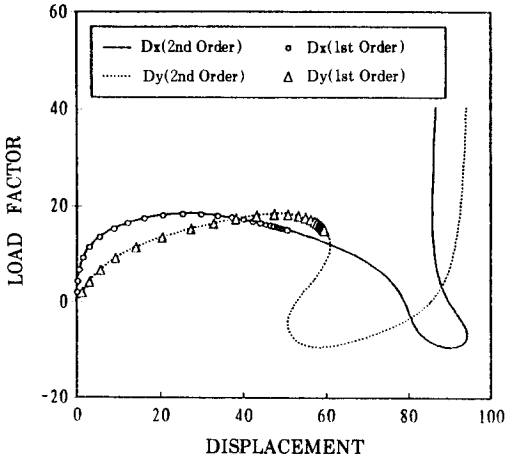

FIG. 5 Comparison of the 1st and 2nd Order Formulation in the Load-Displacement Curve at Point *m*

trace the entire equilibrium path, but the 1st order formulation breaks down after the first load limit point.

4.3 CLAMPED-HINGED CIRCULAR ARCH

Figure 6 shows a schematic representation of a clamped-hinged circular arch subjected to a point load at the center. The arch is modeled by twenty four beam elements. This problem of arch instability after large asymmetric pre-buckling deflections has been investigated by Da Deppo and Schmit[40] and analyzed by Wood and Zienkiewicz[41] and Kouhia and Mikkola.[42]

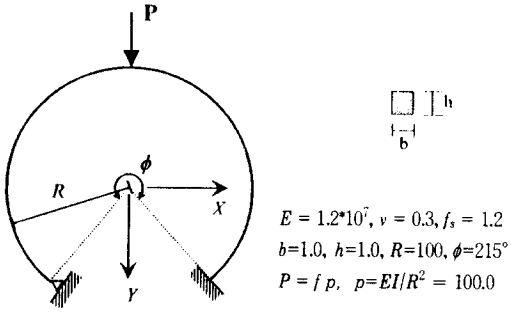

FIG. 6 Clamped-Hinged Circular Arch under a Center Load

The limit loads obtained by this study are compared with those of above researchers in Table 2. This shows that the results of this study agree well with the analytic solution obtained by Da Deppo and Schmit.[40] Figure 7 displays the analyzed results of the load parameter versus the vertical (D_y) and the hori-

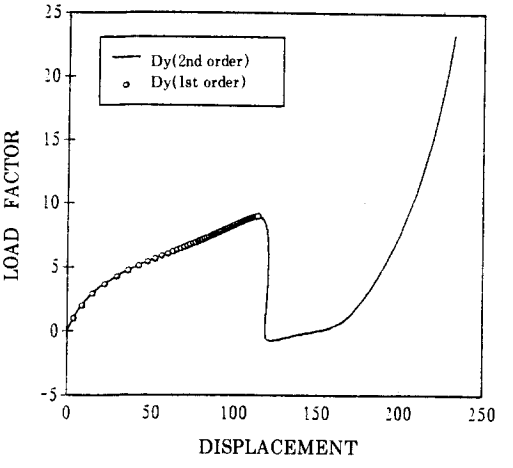

(a) The Load-Vertical Displacement Curve at the Center

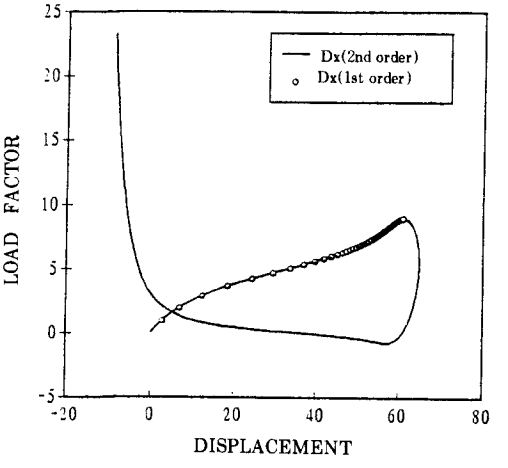

(b) The Load-Horizontal Displacement Curve at the Center

FIG. 7 Comparison of the 1st and 2nd Order Formulation in the Load-Displacement Curves at the Center

zontal (D_x) displacements at the center using the 1st order and the 2nd order formulation. It is found that the 1st order formulation breaks down after the first load limit point, but the 2nd order formulation can trace all equilibrium path with the combined load/displacement method even if the gradient of the curve is very stiff as shown in Figure 7.

Table 2 Limit Loads of Clamped-Hinged Arch

Method \ Limit load	1st Limit Load (EI/R^2)	2nd Limit Load (EI/R^2)
This Study	8.95	-0.73
Analytic Solution[40]	8.97	---
Wood and Zienkiewicz[41]	9.24	---
Kouhia and Mikkola[42]	9.00	-0.76

4.4 HEXAGONAL SPACE FRAME

This problem consists of a three dimensional frame composed of twelve members, with half of them laid out as an hexagon, and the other half making up the diagonals of the hexagon. The load is applied vertically on the central node. To Remove the translational rigid body motions, the central node is restricted against the lateral displacement. Each member of the frame is modeled by two degenerate beam elements.

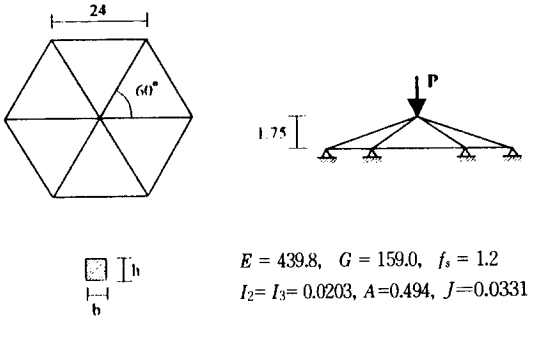

FIG. 8 Hexagonal Space Frame under a Center Load

The evolution of the deflection of the apex, while the load is varied, is given in Figure 9. This represents the typical non-linear behavior with two load limit points. This example is solved by Papadrakakis[43] who has studied on the application of two vector iteration methods in the investigation of the large deflection behavior of spatial structures. Figure 9 shows that both results of the 1st and 2nd order formulations agree well with those of Papadrakakis.[43] From this example, it can be found that the present formulation considering the second order terms of finite rotations shows good results whether the rotation is large or not.

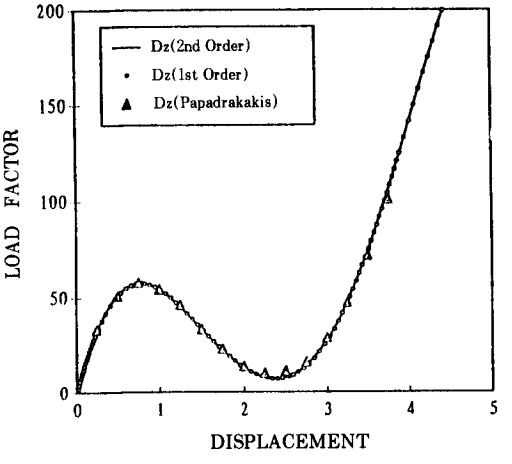

FIG. 9 Load-Vertical Displacement Curves at Apex

5. CONCLUSIONS

A total Lagrangian formulation based on the degenerate beam elements is presented. The strongly geometrically non-linear problems of slender structures are solved by considering the effect of second order terms of finite rotations. In the numerical examples focused on the post-buck-

ling analysis of space frames, the proposed formulation has been compared with the previous works. The results have been shown to be in good agreement with previous works. Also, the proposed formulation has been compared with the formulations assuming infinitesimal rotation increments to verify the effects of finite rotations in the geometrically non-linear analysis of space frames. The results shows that the effects of finite rotations can be found in the problem of the convergence rate, the trace of entire equilibrium path and so on. As a result, the following conclusions are drawn:

1. The initial and deformed configurations of the space frames and the arches can be modeled accurately using the proposed curved beam elements.

2. The post-buckling equilibrium path of the slender structures with multiple limit points can be fully traced by the automatic combination method of load and displacement incrementation with the proposed curved beam element.

3. The present formulation including the second order terms of the incremental rotation shows superiority in the accuracy of results and extremely good convergence characteristics when compared with the formulation including only the first order terms. Therefore, in order to evaluate the tangent stiffness of degenerate beam elements accurately, the second order rotational terms should be included in the non-linear strain terms of the incremental equations, whether the rotation is finite or not.

APPENDIX

From the beam assumption, the strain vectors can be expressed as

$$ {}_oE_L^T = [\, {}_oe_{rr}\ 2{}_oe_{rs}\ 2{}_oe_{rt}\,] \tag{40a} $$

$$ {}_oE_{NL}^T = [\, {}_oU_{r,r}\ {}_oU_{r,s}\ {}_oU_{r,t}\ {}_oU_{s,r}\ {}_oU_{s,s}\ {}_oU_{s,t}\ {}_oU_{t,r}\ {}_oU_{t,s}\ {}_oU_{t,t}\,] \tag{40b} $$

$$ {}_oE_{NL}^{*T} = [\, {}_oe_{rr}^*\ 2{}_oe_{rs}^*\ 2{}_oe_{rt}^*\,] \tag{40c} $$

and the gradient matrix of total displacements ${}_o^tL$ is,

$$ {}_o^tL = \begin{bmatrix} l_{rr} & 0 & 0 & l_{sr} & 0 & 0 & l_{tr} & 0 & 0 \\ l_{rs} & l_{rr} & 0 & l_{ss} & l_{sr} & 0 & l_{ts} & l_{tr} & 0 \\ 0 & l_{rt} & l_{rs} & 0 & l_{st} & l_{ss} & 0 & l_{tt} & l_{ts} \end{bmatrix} \tag{41} $$

where

$$ l_{rs} = {}_o^tU_{r,s} \tag{42} $$

The stress matrix ${}_o^tS$, the stress vector ${}_o^t\bar{S}$, and the constitutive matrix ${}_oC$ are expressed, respectively, as follows

$$ {}_o^tS = \begin{bmatrix} {}^t\widetilde{S} & 0_3 & 0_3 \\ 0_3 & {}^t\widetilde{S} & 0_3 \\ 0_3 & 0_3 & {}^t\widetilde{S} \end{bmatrix} \tag{43} $$

$$ {}_o^t\bar{S}^T = [\, {}_o^tS_{rr},\ {}_o^tS_{rs},\ {}_o^tS_{rt}\,] \tag{44} $$

$$ {}_oC = \begin{bmatrix} E & 0 & 0 \\ & f_{s1}G & 0 \\ sym. & & f_{s2}G \end{bmatrix} \tag{45} $$

where

$$ {}^t\widetilde{S} = \begin{bmatrix} {}_o^tS_{rr} & {}_o^tS_{rs} & {}_o^tS_{rt} \\ {}_o^tS_{sr} & 0 & 0 \\ {}_o^tS_{tr} & 0 & 0 \end{bmatrix} \quad \text{and } 0_3 = \begin{bmatrix} 0 & 0 & 0 \\ 0 & 0 & 0 \\ 0 & 0 & 0 \end{bmatrix} \tag{46} $$

REFERENCES

[1] S. Ahmad, B. M. Irons, and O. C. Zienkiewicz, 1970: Analysis of thick and thin shell structures by curved element, International Journal for Numerical Methods in Engineering, Vol. 2, pp. 419-451.

[2] J. Oliver and E. Oñate, 1984: A total Lagrangian formulation for the geometrically nonlinear analysis of structures using finite elements. Part I. Two-dimensional problems: Shell and plate structures, International Journal for Numerical Methods in Engineering, Vol. 20, pp. 2253-2281.

[3] J. Oliver and E. Oñate, 1986: A total Lagrangian formulation for the geometrically nonlinear analysis of structures using finite elements. Part II. Arches, frames and axisymmetric shells, International Journal for Numerical Methods in Engineering, Vol. 23, pp. 253-274.

[4] K. C. Park and G. M. Stanley, 1986: A curved C shell element based on assumed natural-coordinate strains, Journal of Applied Mechanics, ASME, Vol. 53, pp. 278-290.

[5] K. J. Bathe and E. N. Dvorkin, 1985: A four-node plate bending element based on Mindlin /Reissner plate theory and a mixed interpolation, International Journal for Numerical Methods in Engineering, Vol. 21, pp. 367-383.

[6] K. J. Bathe and E. N. Dvorkin, 1986: A formulation of general shell elements - the use of mixed interpolation of tensorial components, International Journal for Numerical Methods in Engineering, Vol. 22, pp. 692-722.

[7] E. Ramm, 1977: A plate/shell element for large deflections and rotations, Formulations and Computational Algorithms in Finite Element Analysis, U.S.-Germany Symposium, edited by K. J. Bathe, J. T. Oden, and W. Wünderlich, MIT Press, Cambridge, MA.

[8] T. J. R. Hughes, R. L. Taylor, and A. Kanoknukulchai, 1977: A simple and efficient element for plate bending, International Journal for Numerical Methods in Engineering, Vol. 11, pp. 1529-1543.

[9] T. J. R. Hughes and W. K. Liu, 1981: Nonlinear finite element analysis of shells: Part I. Three dimensional shells, Computer Methods in Applied Mechanics and Engineering, Vol. 26, pp. 331-362.

[10] H. Stolarski and T. Belytschko, 1982: Membrane locking and reduced integration for curved elements, Journal of Applied Mechanics, Vol. 49, pp. 172-176.

[11] H. Stolarski and T. Belytschko, 1983: Shear and membrane locking in the curved C° elements, Computational Methods in Applied Mechanics and Engineering, Vol. 41, pp. 279-296.

[12] T. Belytschko, W. K. Liu, J. S. J. Ong and D. Lam, 1985: Implementation and application of a 9-node Lagrange shell element with spurious mode control, Computers and Structures, Vol. 20, No. 1-3, pp. 121-128.

[13] A. F. D. Loula, T. J. R. Hughes and L. P. Franca, 1987: Petrov-Galerkin formulations of the Timoshenko beam problem, Computer Methods in Applied Mechanics and Engineering, Vol. 63, pp. 115-132.

[14] A. F. D. Loula, T. J. R. Hughes, L. P. Franca and I. Miranda, 1987: Mixed Petrov-Galerkin methods for the Timoshenko beam problem, Computer Methods in Applied Mechanics and Engineering, Vol. 63, pp. 133-154.

[15] A. F. D. Loula, T. J. R. Hughes, L. P. Franca and I. Miranda, 1987: Stability, convergence and accuracy of a new finite element methods for the circular arch problem, Computer Methods in Applied Mechanics and Engineering, Vol. 63, pp. 281-303.

[16] T. J. R. Hughes and L. P. Franca, 1988: A mixed finite element formulation for Reissener- Mindlin plate theory-uniform convergence of all higher-order spaces, Computer Methods in Applied Mechanics and Engineering, Vol. 67, pp. 223-240.

[17] F. Brezzi, M. O. Bristeau, L. P. Franca, M. Mallet and G. Roge, 1992: A relationship be-

tween stabilized finite element methods and the Galerkin method with bubble functions, Computer Methods in Applied Mechanics and Engineering, Vol. 96, pp. 117-129.

[18] O. C. Zienkiewicz and E. Hinton, 1976: Reduced integration, function smoothing and nonconformity in finite element analysis (with special reference to thick plates), Journal of the Franklin Institute, Vol. 302, pp. 443-461.

[19] E. D. L. Pugh, E. Hinton and O. C. Zienkiewicz, 1978: A study of quadrilateral plate bending elements with reduced integration, International Journal for Numerical Methods in Engineering, Vol. 12, pp. 1059-1079.

[20] T. J. R. Hughes, M. Cohen and M. Haroun, 1978: Reduced and selective integration techniques in the finite element analysis of structures, Nuclear Engineering and Design, Vol. 46, pp. 445-450.

[21] A. K. Noor and C. M. Anderson, 1981: Mixed models and reduced/selective integration displacement models for nonlinear shell analysis, Nonlinear Finite Element Analysis, edited by T. J. R. Hughes, A. Pifko and A. Jay, Proceedings of the ASME Winter Annual Meeting, AMD-Vol. 48.

[22] O. P. Jacquotte and J. T. Oden, 1984: Analysis and treatment of Hourglass instabilities in underintegrated finite element methods, Proceedings of the International Conference on Innovative Methods for Nonlinear Analysis, edited by W. K. Liu, T. Belytschko, and K. C. Park, 1984, Prineridge Press International Ltd., Swansea, Wales, UK.

[23] W. K. Liu, T. Belytschko and J. S. J. Ong, 1984: The use of stabilization matrices in nonlinear analysis, Proceedings of the International Conference on Innovative Methods for Nonlinear Problems, edited by W. K. Liu, T. Belytschko, and K. C. Park, 1984, Prineridge Press International Ltd., Swansea, Wales, UK.

[24] K. J. Bathe, 1996: Finite Element Procedures in Engineering Analysis, Prentice-Hall.

[25] K. J. Bathe and S. Bolourichi, 1979: Large displacement analysis of three-dimensional beam structure, International Journal for Numerical Methods and Engineering, Vol. 14, pp. 961-986.

[26] J. Argyris, 1982: An excursion into large rotations, Computer Methods in Applied Mechanics and Engineering, Vol. 32, pp. 85-155.

[27] K. S. Surana, 1983: Geometrically nonlinear formulation for the curved shell elements, International Journal for Numerical Methods in Engineering, Vol. 19, pp. 581-615.

[28] K. S. Surana, 1983: Geometrically non-linear formulation for two dimensional curved beam elements, Computers & Structures, Vol. 17, No. 1, pp. 105-114.

[29] K. S. Surana and R. M. Sorem, 1989: Geometrically non-linear formulation for three dimensional curved beam elements with large rotations, International Journal for Numerical Methods in Engineering, Vol. 28, pp. 43-73.

[30] E. N. Dvorkin, E. Oñate and J. Oliver, 1988: On a non-linear formulation for curved Timoshenko beam elements considering large displacement/rotation increments, International Journal for Numerical Methods in Engineering, Vol. 26, pp. 1957-1613.

[31] J. C. Simo, 1985: A finite strain beam formulation. The three-dimensional dynamic problem. Part I, Computer Methods in Applied Mechanics and Engineering, Vol. 32, pp. 55-70.

[32] J. C. Simo and L. Vu Quoc, 1986: A three dimensional finite strain rod model. Part II: computational aspects, Computer Methods in Applied Mechanics and Engineering, Vol. 58, pp. 79-116.

[33] M. A. Crisfield, 1981: A fast incremental/iterative solution procedure that handles 'snap-through', Computers & Structures, Vol. 13, pp. 55-62.

[34] K. J. Bathe and E. N. Dvorkin, 1983: On the automatic solution of nonlinear finite element equations, Computers & Structures,

Vol. 17, pp. 871-879.

[35] P. X. Bellini and A. Chulya, 1987: An improved automatic incremental algorithm for the efficient solution of nonlinear finite element equations, Computers & Structures, Vol. 26, pp. 99-110.

[36] M. Y. Kim and S. P. Chang, 1990: Geometric non-linear finite element analysis of the space truss, Journal of Korean Society of Steel Construction, Vol. 2, pp. 164-174.

[37] M. Y. Kim and S. P. Chang, 1990: Geometric non-linear analysis of plane frame structures subjected to conservative and non-conservative forces, Journal of Korean Society of Civil Engineers, Vol. 10, pp. 17-26.

[38] M. Y. Kim and S. P. Chang, 1990: Automatic load and displacement incremental algorithm for geometric non-linear finite element analysis of the structure subjected to conservative and non-conservative forces, Journal of Korean Society of Civil Engineers, Vol. 10, pp. 164-174.

[39] C. Cichon, 1984: Large displacements in-plane analysis of elastic-plastic frames, Computers & Structures, Vol. 19, No. 5/6, pp. 737-745.

[40] D. A. Da Deppo and R. Schmidt, 1975: Instability of clamped-hinged circular arches subjected to a point load, Transactions of ASME, pp. 894-896.

[41] R. D. Wood and O. C. Zienkiewicz, 1977: Geometrically non-linear finite element analysis of beams, frames, arches and axisymmetric shells, Computers & Structures, Vol. 7, pp. 725-735.

[42] R. Kouhia and M. Mikkola, 1989: Tracing the equilibrium path beyond simple critical points, International Journal for Numerical Methods in Engineering, Vol. 28, pp. 2923-2941.

[43] M. Papadrakakis, 1981: Post-buckling analysis of spatial structures by vector iteration methods, Computers & Structures, Vol. 14, No. 14, pp. 393-402.